

RESEARCH ARTICLE

Glycation of H1 Histone by 3-Deoxyglucosone: Effects on Protein Structure and Generation of Different Advanced Glycation End Products

Jalaluddin Mohammad Ashraf^{1*}, Gulam Rabbani², Saheem Ahmad³, Qambar Hasan¹, Rizwan Hasan Khan², Khursheed Alam⁴, Inho Choi^{1*}

1 School of Biotechnology, Yeungnam University, Gyeongsan, Republic of Korea, **2** Interdisciplinary Biotechnology Unit, Aligarh Muslim University, Aligarh, India, **3** Department of Biotechnology, Integral University, Lucknow, India, **4** Department of Biochemistry, Jawaharlal Nehru Medical College, Aligarh Muslim University, Aligarh, India

* jmashraf@gmail.com (JMA); inchoi@ynu.ac.kr (IC)



OPEN ACCESS

Citation: Ashraf JM, Rabbani G, Ahmad S, Hasan Q, Khan RH, Alam K, et al. (2015) Glycation of H1 Histone by 3-Deoxyglucosone: Effects on Protein Structure and Generation of Different Advanced Glycation End Products. PLoS ONE 10(6): e0130630. doi:10.1371/journal.pone.0130630

Editor: Vladimir N. Uversky, University of South Florida College of Medicine, UNITED STATES

Received: March 11, 2015

Accepted: May 21, 2015

Published: June 29, 2015

Copyright: © 2015 Ashraf et al. This is an open access article distributed under the terms of the [Creative Commons Attribution License](https://creativecommons.org/licenses/by/4.0/), which permits unrestricted use, distribution, and reproduction in any medium, provided the original author and source are credited.

Data Availability Statement: All relevant data are within the paper and its Supporting Information files.

Funding: This study was supported by a National Research Foundation of Korea grant funded by the Republic of Korea government (MSIP; no. 2014R1A2A2A01006324).

Competing Interests: The authors have declared that no competing interests exist.

Abstract

Advanced glycation end products (AGEs) culminate from the non-enzymatic reaction between a free carbonyl group of a reducing sugar and free amino group of proteins. 3-deoxyglucosone (3-DG) is one of the dicarbonyl species that rapidly forms several protein-AGE complexes that are believed to be involved in the pathogenesis of several diseases, particularly diabetic complications. In this study, the generation of AGEs (N^ε-carboxymethyl lysine and pentosidine) by 3-DG in H1 histone protein was characterized by evaluating extent of side chain modification (lysine and arginine) and formation of Amadori products as well as carbonyl contents using several physicochemical techniques. Results strongly suggested that 3-DG is a potent glycating agent that forms various intermediates and AGEs during glycation reactions and affects the secondary structure of the H1 protein. Structural changes and AGE formation may influence the function of H1 histone and compromise chromatin structures in cases of secondary diabetic complications.

Introduction

Advanced glycation end products (AGEs) are a heterogeneous group of complex molecules that include reactive derivatives generated during the non-enzymatic glycation process in which reducing sugars react with the free amino groups of amino acids, proteins, lipoproteins, and nucleic acids. The formation of a reversible Schiff base followed by the creation of covalently bound Amadori products along with a series of chemical reactions results in the irreversible formation of heterogeneous complex compounds known as AGEs [1]. Enhanced AGE development in cases of chronic hyperglycemia due to an increased rate of non-enzymatic glycation of macromolecules is known to cause tissue injuries and consequently aggravate secondary diabetic complications [2–4].

Previously, glucose was regarded as the major instigator of AGEs formation but several other sugar and non-sugar compounds have been found to be more reactive than glucose [5–8]. Among the non-sugar compounds, endogenous α -dicarbonyls are powerful glycation agents responsible for the generation of carbonyl stress, especially under diabetic conditions [9]. Indigenous α -dicarbonyl intermediates are formed through various mechanisms and pathways such as the glycolytic pathway, auto-oxidation of glucose, during all stages of Maillard reaction, and lipid peroxidation [10–13]. These entities are very reactive (20,000 times that of reducing sugars), and react swiftly with arginine and lysine residues on proteins; thus, AGEs can be formed even with extremely low concentrations of α -dicarbonyls [14, 15]. Among the α -dicarbonyls, 3-deoxyglucosone (3-DG), methylglyoxal (MG), and glyoxal are the major precursors of AGEs [16, 17]. 3-DG levels are elevated in patients with diabetes [18], and its role in the development of secondary diabetic complications has been reported [19].

Transcriptional activity of genes depends upon the packaging of chromatin by histone proteins [20]. Histones have been found to play important roles in the epigenetic regulation of gene expression [21, 22]. In particular, the linker histone (H1) is important for chromatin organization and the regulation of gene expression [23].

Several studies have demonstrated that histones are significantly vulnerable to nonenzymatic glycation. Gugliucci [24] provides evidence for the *in vitro* formation of both pentosidine and AGEs on histones. The same group revealed three folds higher AGE level in histones isolated from the liver of diabetic rats [25]. A similar result was also observed in diabetic patients [26]. *In vitro* analysis also showed glycation and glycooxidation of histone with ADP-ribose [27]. In the same way, mass spectrometry-based study of histones H1 and H2B has showed “glycooxidative” damage at different position and all of the identified glycated positions in both histones were lysine residues, [28, 29]. Recently, Talaz and co-workers [30] demonstrated the formation of AGEs *in vitro* glycation of H1 histones, core histones or total histones proteins with several sugars (glucose, ribose and fructose). Moreover, quite recent studies have shown the formation of AGEs by glycation of whole histones and H2A histone with methylglyoxal resulting in structural alteration in the proteins [31, 32]. Recently, we also produced evidence of AGE formation as well as structural change on histones *in vitro* [33, 34].

Because of the following factors, including permeability of nuclear membrane for lower weight molecules up to 5 kDa, peripheral position of histone H1 in chromatin, high content of lysine in H1 and long half life of this histone (4–5 month) make the H1 highly prone to be attacked by glycation agents. Being a small molecule, 3-DG can easily diffuse in nuclear membrane in turn can damage nuclear proteins by glycation it. To date, no extensive studies have been conducted to assess the glycation of H1 proteins by 3-DG. Therefore, the present study was conducted to examine the ability of 3-DG to glycate H1 histone protein. Generation of AGEs in H1 protein by 3-DG and secondary structural changes in the 3-DG-glycated H1 protein were evaluated by various physicochemical techniques.

Materials and Methods

Chemicals

3-DG, arginine, lysine, calf thymus H1 histone protein, sodium azide; 9,10-phenanthrenequinone, 2,4-dinitrophenyl hydrazine (DNPH); dialysis tubing, and other reagents/chemicals were obtained from Sigma Chemical Company (St. Louis, MO, USA). Nitroblue tetrazolium (NBT) was from Sisco Research Laboratories (India).

Histone glycation by 3-DG

The glycation of calf thymus H1 histone (1 mg/mL) was carried out by incubation with 10 μ M 3-DG and 10 mM sodium phosphate saline buffer (pH 7.4) at 37°C for 14 day. Native H1 histone was incubated under the same conditions but without 3-DG as a control. Dialysis was performed at 4°C against sodium phosphate saline buffer at pH 7.4 to remove unreacted 3-DG in the solution. The samples were stored at -80°C for later use.

Assessment of free amino groups by a fluorescamine assay

Lysine side chain modifications were evaluated with a fluorescamine assay as previously described with slight modification [35–37]. Briefly, 5 μ L (1 mg/mL) of a solution containing 3-DG-glycated H1 histone, 100 μ L of 100 mM Na₂HPO₄, 45 μ L aqua dest, and 50 μ L fluorescamine reagent (1 mM fluorescamine in acetonitrile) were mixed and incubated for 10 min in the dark at room temperature. Fluorescence of the sample was measured at excitation/emission wavelengths of 390/490 nm on FLUORO-STAR plate reader (BMG, Germany). N- α -acetyl-lysine at concentrations of 0 to 1.5 mM was used as the standard to determine the lysine content of the protein solution. Fresh H1 protein (1 mg/mL) and PBS solution were used as controls for AGE-H1 histone and background fluorescence, respectively.

Examination of free arginine side chains with a 9,10-phenanthrenequinone assay

Free arginine content was measured as previously described [38, 37]. Briefly, 50 μ L of H1 protein (1 mg/mL) was mixed with 150 μ L (150 μ M) of 9,10-phenanthrenequinone reagent (dissolved in 100% ethanol) followed by the addition of 25 μ L NaOH (2 N). The final reaction containing the proteins minus 9,10-phenanthrenequinone was used to correct the AGE fluorescence results. 3-DG-glycated H1 protein was incubated at 60°C for 3 h after which 40 μ L of the reaction was transferred to a multiple-well plate and mixed with 40 μ L of 1.2 N HCl. Fluorescence was measured at excitation/emission wavelengths of 312/395 nm after incubating the samples for 1 h in the dark at 25°C on FLUORO-STAR plate reader (BMG, Germany). N- α -acetyl-arginine (0 to 0.4 mM) was used as a standard to measure the arginine content. H1 histone (1 mg/mL) and PBS solution were used as controls for the AGE-H1 histone and background fluorescence, respectively.

Detection of Amadori products in 3-DG-glycated H1 histone

NBT dye was used to detect Amadori product (fructosamine) in the 3-DG-glycated H1 protein as previously described with minor modification [39, 33]. Briefly, samples were mixed at a ratio of 1:10 with sodium carbonate-bicarbonate buffer (100 mM, pH 10.8) containing 0.25 mM NBT and then incubated at 37°C for 45 min. Absorbance was measured at 525 nm relative to distilled water. Amadori product concentration (nM/mL) was determined by multiplying the absorbance by a molar extinction coefficient of 12.64.

Evaluation of carbonyl contents

Carbonyl contents of native and 3-DG-glycated H1 histone samples were determined as previously described with slight modifications [40, 33]. Briefly, 15 μ M 3-DG-glycated and native H1 histones were dissolved in 10 mM 2,4-dinitrophenyl hydrazine (DNPH) solution in 2 N HCl. The samples were then vortexed for 1 h at room temperature, subjected to precipitation with 0.5 mL of 20% (v/v) TCA (Trichloroacetic acid), and centrifuged at 11,000 \times g for 3 min at 4°C.

The resulting pellet was washed with 1 mL of an ethanol-ethyl acetic acid mixture (1:1; v:v) to remove extra DNPH reagent. Next, the samples were incubated at room temperature for 10 min, and then centrifuged at $11,000 \times g$ for 5 min at 4°C. The pellet was washed twice with the ethanol-ethyl acetic acid mixture and suspended in 1 mL of 6 M guanidium hydrochloride dissolved in 20 mM potassium phosphate buffer (pH 2.3, adjusted with trifluoroacetic acid). The samples were subsequently incubated at 37°C for 15–30 min to dissolve the proteins. Carbonyl contents in the supernatant were measured relative to 6 M guanidium hydrochloride (as a blank) using a molar extinction coefficient of $22,000 \text{ M}^{-1} \text{ cm}^{-1}$ at 370 nm. Protein carbonyl contents were expressed as nmol/mg of protein.

Evaluation of carboxymethyl lysine (CML) content by an ELISA

CML generation was measured with an ELISA as described previously with slight modification [41, 37] using 2,2'-azinobis (3-ethylbenzothiazoline-6-sulfonic acid) as the detection agent [S1 Fig]. A solution containing native H1 protein (1 mg/mL) and PBS were used as controls. An ELX800 multi-well plate reader (BioTek Instruments, USA) measured the absorbance of the samples at 405 nm.

Determination of AGE-CML and pentosidine with a chromatographic assay

CML and pentosidine concentrations in the sample were estimated by high performance liquid chromatography (HPLC) as previously described [42, 33]. For enzymatic hydrolysis, all procedures were carried out under nitrogen. Briefly, 100 µg of samples were diluted with 20 µL of water followed by the addition of 25 µL (40 mM) HCl, 5 µL of a pepsin solution (2 mg/mL in 20 mM HCl), and 5 µL of a thymol solution (2 mg/mL in 20 mM HCl). The samples were incubated at 37°C for 24 h. The reactions were then neutralized with 25 µL of 0.5 M potassium phosphate buffer (pH 7.4) and 5 µL (260 mM) KOH. Next, 5 µL of pronase E (2 mg/mL in 10 mM KH_2PO_4 , pH 7.4) were added and the reactions were incubated at 37°C for 24 h. Subsequently, 5 µL of an aminopeptidase solution (2 mg/mL in 10 mM KH_2PO_4 , pH 7.4) and 5 µL of a prolidase solution (2 mg/mL in 10 mM KH_2PO_4 , pH 7.4) were added, and the samples were incubated at 37°C for 48 h. Afterward, 50 µL enzymatic hydrolysate (equivalent to 50 µg of protein) were placed in 1-mL glass vials, and 10 µL internal standard (α -aminobutyric acid, 100 nmol/mL), 40 µL water, 100 µL aminoquinolyl-N-hydroxysuccinimidyl-carbamate (AQC) derivatizing buffer (500 mM borate buffer and 400 µM DTPA, pH 8.8), and 200 µL AQC (6-Aminoquinolyl-N-hydroxysuccinimidylcarbamate) (10 mM in acetonitrile) were added. Calibration standards contained AGE standards (0–1000 pM) and amino acids (0–20 nM). The test and calibration standard samples were incubated at 55°C for 10 min after which the samples were lyophilized and reconstituted in 100 µL water. AQC-labelled hydrolysates were filtered by centrifugal filtration (0.2-µm pore) and the filtrates were then analyzed by reverse-phase HPLC. The Waters 600 HPLC system (Water scientific, USA) consisted of a Waters 717 plus auto-sampler that maintained sample temperature at 18°C, Waters 600 quaternary pump, Waters 474 fluorescence detector, and Waters 481 Lambda Max absorbance detector in series. A 2-channel data collection system (Kontron) and a flow rate of 1 mL/min were used for analysis. Calibration curves for the amino acids (0–20 nM) and AGE (0–1 nM) were constructed, and 25 µg of the control and glycated proteins were analyzed. The detection limits were 2–20 pM and the inter batch coefficients of variation ranged from 4–29% depending on the analyte. All analytical recoveries exceeded 90%.

HPLC analysis

CML and pentosidine contents in native H1 and 3-DG-glycated H1 samples were analyzed by HPLC as previously described [43]. Briefly, the samples were first hydrolyzed with 6 N HCl for 24 h at 110°C. The hydrolyzed samples were then passed through a 0.42- μ m Millex filter for ultrafiltration. The filtered samples were analyzed with an ion exchange HPLC column (2622 SC, 4.6 \times 60 mm; Hitachi, Japan). The retention times of CML and pentosidine standards were measured as a reference.

Spectroscopic analysis

UV absorbance of native and 3-DG-glycated H1 was recorded with a Perkin Elmer (Shelton, CT, USA) Lambda 25 spectrophotometer at a wavelength range of 200–400 nm [44, 33]. Percent increase of hyperchromicity was calculated with the following formula:

$$\% \text{ increase hyperchromicity} = \frac{\text{Abs. of glycated H1} - \text{Abs. of native H1}}{\text{Abs. of glycated H1}} \times 100$$

Fluorescence analysis

Fluorescence characteristics of native and 3-DG-glycated H1 were investigated with a Hitachi spectrofluorometer (F-4500). A quartz cuvette with a 1-cm pathlength was used for the experiments. Emission profiles of the samples were recorded at excitation wavelengths of 335 and 365 nm [44, 33]. Percent increase in the fluorescence intensity (FI) was calculated with the following formula:

$$\% \text{ increase FI} = \frac{\text{FI of glycated H1} - \text{FI of native H1}}{\text{FI of glycated H1}} \times 100$$

Circular dichroism (CD) measurements

A CD spectral study was performed with a Jasco spectropolarimeter, J-815 (Jasco, Japan) coupled with a Jasco Peltier-type temperature controller (PTC-424S/15). The instrument was calibrated with D-10-camphorsulphonic acid and measurements were carried out at 25°C using a temperature-controlled cell holder attached to a Neslab RTE water bath with an accuracy of $\pm 0.1^\circ\text{C}$. Spectral profiles of the samples (20 μM) were obtained with 1-mm pathlength cuvettes at a wavelength range of 200–250 nm. A scan speed of 100 nm/min and response time of 1 sec was selected to record the CD spectra. Two sets of each sample were analyzed under the same conditions to confirm reproducibility of the results. Furthermore, thermal unfolding of native and 3-DG-glycated H1 was evaluated by measuring the temperature-dependent CD response at 208 nm from 25–90°C at a temperature increase of 1°C/min [45, 33].

Fourier transformed-infra red (FT-IR) spectroscopy

Structural alteration of 3-DG-glycated H1 was characterized by FT-IR spectroscopy. Transmission spectra were recorded over 600–4000 cm^{-1} with a Spectrum 100 FTIR spectrometer (Perkin Elmer) as previously described [33].

Results

Formation of intermediates during glycation

Free amino groups in lysine and arginine residues of native and 3-DG-glycated H1 histone were identified by fluorescamine and 9,10-phenanthrenequinone assays, respectively. The percentage of reacted lysine and arginine residues was 85.50 and 78.30% in 3-DG-glycated H1, respectively. Amadori product formation during the glycation reaction was estimated by reduction of the NBT dye. During this process, yellow NBT dye is converted to purple monoformazan, indicating the formation of Amadori products. On day 6, the maximum amount of Amadori product (12.03 ± 1.32 nM/mL) was observed in 3-DG-glycated H1. Carboxylation of lysine, arginine, threonine, and proline residues is a characteristic marker of protein oxidation. 3-DG-mediated oxidation may lead to the modification of the amino acid side chains. The carbonyl content in the 3-DG-glycated H1 sample was 23.23 ± 1.56 nmol/mg protein, while that in native H1 was 5.33 ± 0.78 nmol/mg protein. All results are summarized in [Table 1](#).

Determination AGE formation by an ELISA and HPLC analysis

The CML content in native and 3-DG-glycated H1 was evaluated by ELISA immunoassay. 3-DG-glycated H1 contained 1.87 ± 0.20 nM/ml amount of CML, whereas negligible amount of CML content was observed in native H1. Significant amounts of CML and pentosidine were identified in enzymatically hydrolyzed 3-DG-glycated H1. The CML and pentosidine contents in 3-DG-glycated H1 were 1.73 ± 0.05 and 1.06 ± 0.08 nM/ml, respectively. These results are summarized in [Table 1](#).

HPLC was used to substantiate the formation of CML and pentosidine in acid hydrolyzed native and 3-DG-glycated H1. The chromatogram of native H1 did not contain any peak corresponding to standard CML or pentosidine (used as references; [Fig 1A](#)). The standard CML and pentosidine corresponded to separate peaks with retention times of 21.42 and 24.12 min, respectively ([Fig 1B and 1C](#)). Two major peaks with retention time of 23.35 and 24.18 min that correspond to standard CML and pentosidine, respectively, were observed for 3-DG-glycated H1 ([Fig 1D](#)).

Observation of AGE formation in 3-DG-glycated H1 histone by spectroscopic analysis

Pilot experiments were carried out to determine the optimum concentration of 3-DG needed to modify histone protein. Briefly, 3-DG (10 μ M) was mixed with H1 (1 mg/mL) and incubated at 37°C for 14 day. Native H1 produced a prominent absorbance peak at 276 nm ([Fig 2](#)). A 93.74% increase in absorbance (hyperchromicity) at 276 nm as well as increased absorbance between 300 to 400 nm was observed for 3-DG-glycated H1. Assessment of fluorescent pentosidine and formation of different AGEs in 3-DG-glycated H1 histone was investigated by exciting the samples at 335 and 365 nm [46]. 3-DG-glycated H1 had a 93.37% increase in emission intensity at λ_{em} 395 nm relative to native H1 upon excitation at λ_{ex} 335 nm ([Fig 3A](#)). The

Table 1. Formation of various intermediates and AGEs.

Sample	Lysine reacted (%)	Arginine reacted (%)	Carbonyl, nM/mg H1	CML, nM/ml H1 (ELISA)	CML, nM/ml H1 (HPLC)	Pentosidine nM/ml H1	Amadori product (nM/ml)
Native H1	-	-	5.33 ± 0.78	0	0	0	0
3-DG-glycated H1	85.50	78.30	23.23 ± 1.56	1.87 ± 0.20	1.73 ± 0.05	1.06 ± 0.08	12.03 ± 1.32

doi:10.1371/journal.pone.0130630.t001

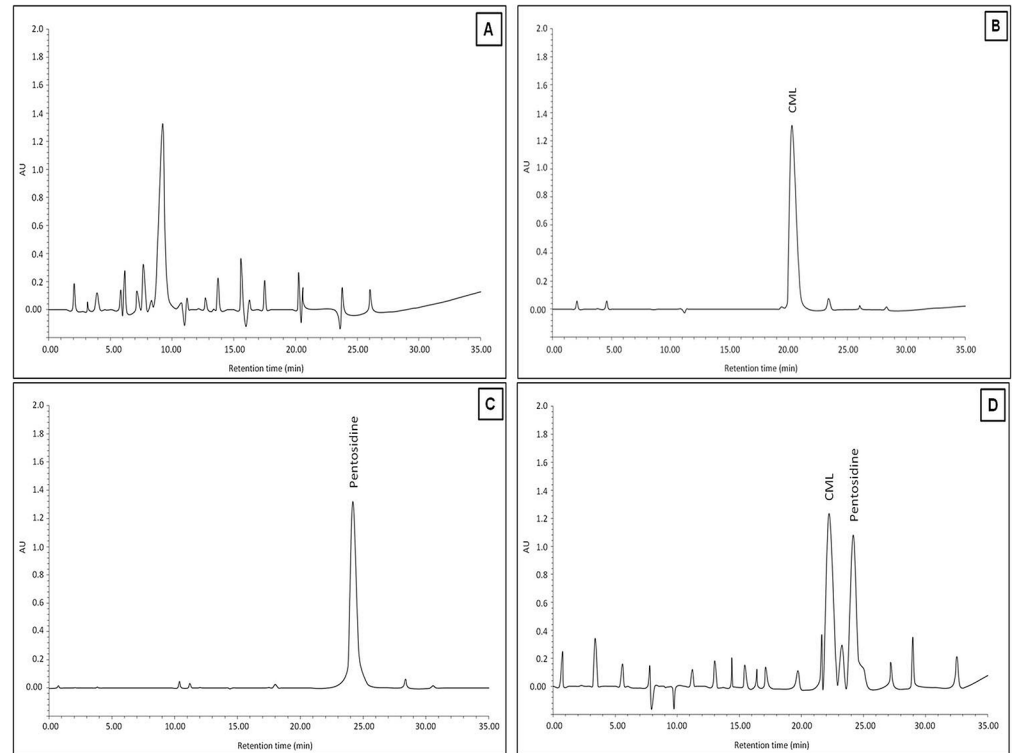


Fig 1. HPLC study of native and 3-DG-glycated H1 histone protein. (A) Chromatograms for native H1, (B and C) standard CML and pentosidine, and (D) glycated H1 protein.

doi:10.1371/journal.pone.0130630.g001

increase in fluorescence intensity at λ_{em} 395 nm for H1 glycated with 3-DG suggests the generation of pentosidine. When the same sample was again excited at 365 nm, a 96.48% increase in fluorescence intensity for glycated H1 histone was observed at λ_{em} 445 nm relative to native H1 histone (Fig 3B). Native H1 showed negligible fluorescence intensity in both cases.

Analysis of structural alteration in 3-DG-glycated H1 protein

CD is a powerful technique used for predicting secondary structure/conformational changes in proteins. In the present study, the characteristic CD properties of proteins were evaluated to investigate the secondary structure of native H1 and subsequent changes after modification with 3-DG. Proteins rich in α -helices produce negative bands at 222 and 208 nm. The 3-DG-glycated H1 histone had a significant decrease in ellipticity at 222 and 208 nm compared to the non-glycated counterpart (Fig 4). This decrease in ellipticity suggests that the secondary structure/conformation of 3-DG-glycated H1 was altered. Thermal unfolding was performed to check the thermodynamic stability of 3-DG-glycated H1 at 222 nm and demonstrate the presence of residual secondary structures in the protein. As shown in Fig 5, the mid-point temperature (T_m) of native H1 was 63.51°C and glycation of native H1 histone by 3-DG resulted in a significant T_m decrease (8.88°C). This significant reduction in T_m indicated a decrease in thermo stability resulting from structural changes in the 3-DG-glycated H1 protein.

FT-IR is also a sensitive technique for examining secondary structural changes in proteins. The FT-IR spectra contains two transmittance bands (amide I, C = O; amide II, N-H bonds) in the range of 1500–1700 cm^{-1} . The two bands are sensitive parameters that are used to predict secondary structural changes in proteins caused by chemical agents [47]. Two transmittance

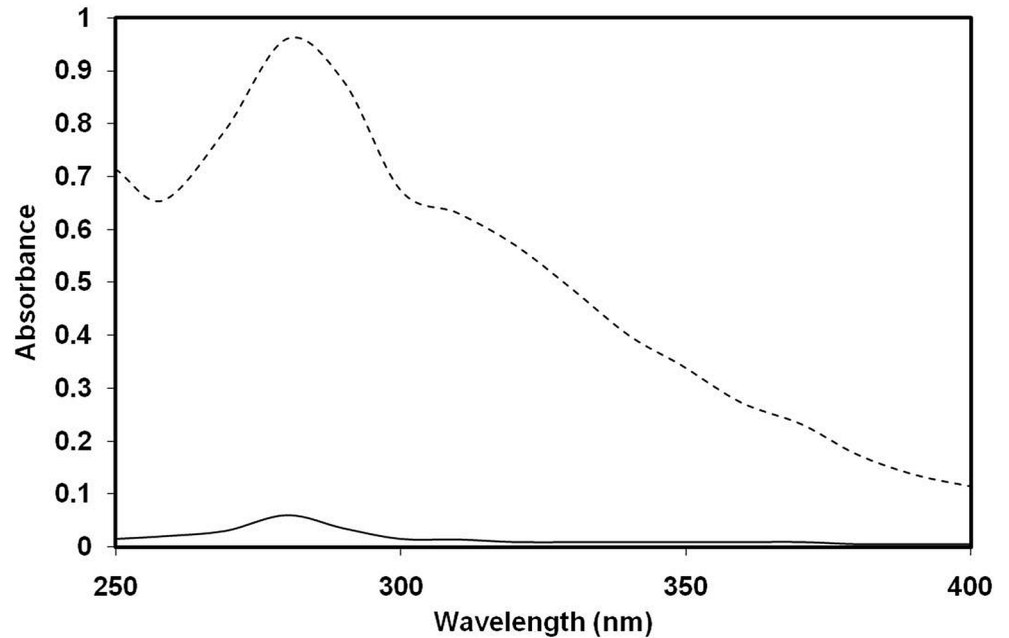


Fig 2. UV-Vis spectral profiles of native (—) and 3-DG- glycated H1 histone (- - -).

doi:10.1371/journal.pone.0130630.g002

bands at 1651 (amide I) and 1542 cm^{-1} (amide II) were observed for native H1. After glycation, the band positions shifted to 1657 (amide I) and 1546 cm^{-1} (amide II) in the spectra (Fig 6).

Discussion

Non-enzymatic glycation of proteins has been widely investigated and found to play a principal role in human physiology and metabolic disorders [48]. High levels of AGEs in the body are associated with a large number of diseases including secondary complications of diabetes, renal failure, and Alzheimer’s disease [49, 50]. 3-DG concentration has been reported to be higher in diabetic subjects, and AGEs consequently play a major role in the initiation and/or progression of diabetic complications [51, 52].

H1 protein is associated with DNA stretch, links nucleosome cores, and promotes the condensation of chromatin [53, 54]. A high lysine and arginine content (30%) makes it more

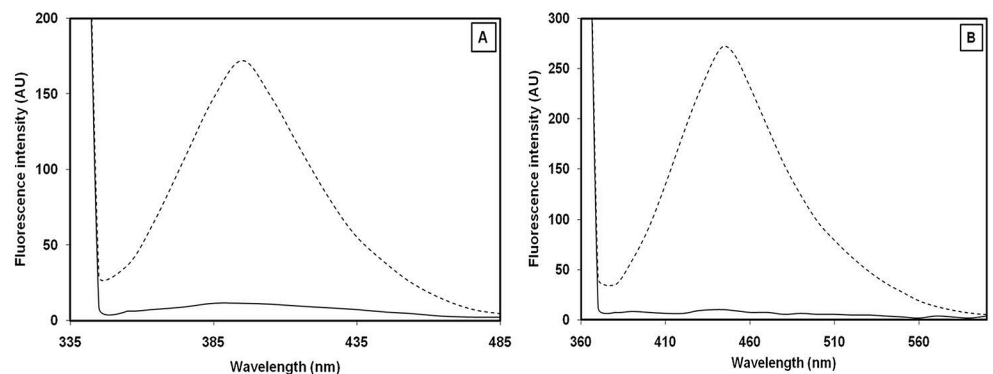


Fig 3. Fluorescence spectral profiles of native (—) and 3-DG-glycated H1 histone (- - -) excited at (A) 335 and (B) 365 nm.

doi:10.1371/journal.pone.0130630.g003

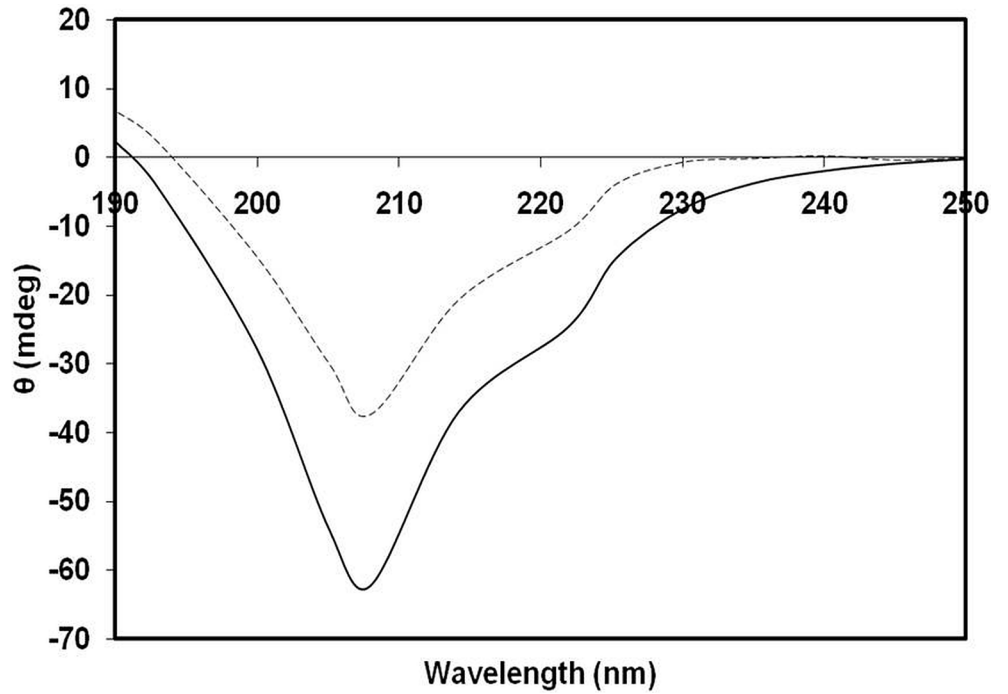


Fig 4. Far-UV CD spectra of native (—) and 3-DG-glycated H1 histone (- - -). The spectra were recorded between 200 and 250 nm. The protein concentration was 0.5 mg/ml and the path-length was 1.0 cm.

doi:10.1371/journal.pone.0130630.g004

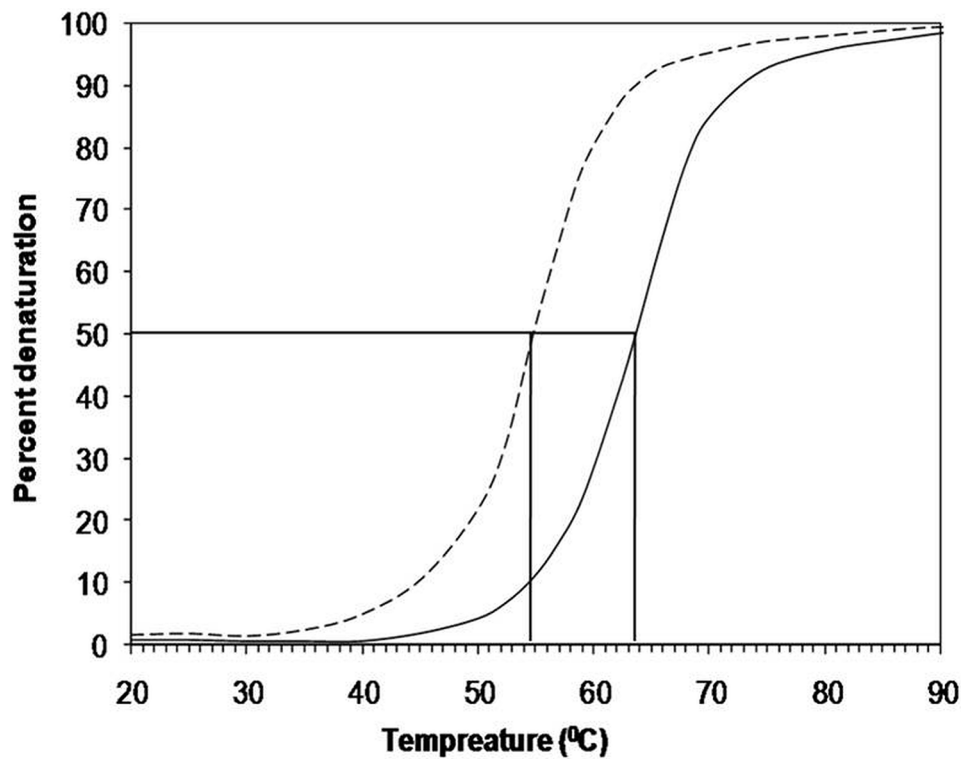


Fig 5. Temperature-induced denaturation spectral profiles demonstrating alteration in ellipticity at 208 nm of native (—) and 3-DG-glycated H1 histone (---).

doi:10.1371/journal.pone.0130630.g005

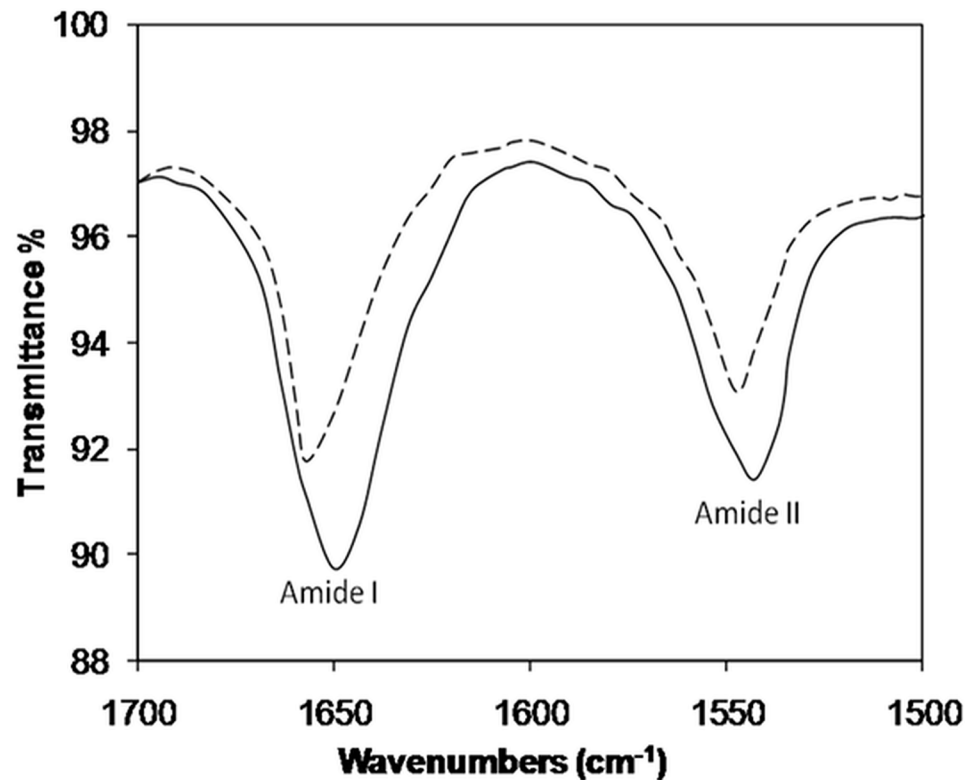


Fig 6. FTIR spectral profiles of Amide I and Amide II bands corresponding to native H3 histones and 3-DG-glycated H3 histone.

doi:10.1371/journal.pone.0130630.g006

susceptible to glycation [55]. In the present study, the ability of 3-DG to glycate H1 histone was investigated by measuring various parameters that indicate the formation of AGEs.

In our study, extent of reactivity of lysine and arginine residue indicates glycating potential of 3-DG with histone protein. Furthermore, the presence of Amadori products and carbonyl contents in 3-DG-modified H1 histone confirms the occurrence of glycation reaction. Previous study has shown that the presence of carbonyl contents point towards the oxidative modifications of proteins during the glycation reaction [56], and the presence of Amadori products signifies that the glycation reaction in its early stage [36, 40, 57]. In short, reactivity of lysine and arginine, carbonyl contents, and Amadori products detected in the reaction system are suggestive of AGE formation. Significant amounts of CML and pentosidine identified by HPLC and ELISA validate the 3-DG capacity in AGE formation. HPLC chromatogram again confirmed the formation of AGEs (CML and pentosidine), as presence of corresponding peaks to standard CML and pentosidine were observed in glycated-H1 protein.

Further fluorescence spectroscopic analysis of the samples again verified the formation of AGEs. The immense increase in fluorescence intensity observed at λ_{em} 396 nm upon excitation at λ_{ex} 335 nm suggested the formation of pentosidine during glycation [37]. Earlier study has reported that glycated arginine and lysine side chains play a key role in the formation of cross-linkage resulting in the development of pentosidine [58]. It is well documented that excitation/emission wavelengths of pentosidine are around 325–335/375–385 nm, substantiating the findings of the current study [59]. The same sample showing considerably increased fluorescence intensity emission wavelength of λ_{em} 445 nm upon excitation at λ_{ex} 365 nm indicated the formation of different AGEs with different excitation/emission wavelengths [60].

The UV absorbance profile of 3-DG-glycated H1 showed significant enhancement of absorbance (hyperchromicity) at 276 nm. This hyperchromicity could be ascribed to exposure of the chromophoric group or generation of more chromophoric groups during the glycation process. The hyperchromicity and increase in absorbance between 300 and 400 nm observed in H1 protein glycated by 3-DG are indicative of glycation taking place that leads to AGE formation [61]. These spectroscopic characteristics of macromolecules (DNA and proteins) have been attributed to glycation occurring under pathophysiological conditions like diabetes, cancer, and atherosclerosis [62–65]. Previous studies of increased absorbance in the range of 300–400 nm have been utilised to predict the formation of AGEs [16, 66].

The effect of glycation on the secondary structure of H1 histone protein was also investigated by CD and FTIR. Two minima, one at 208 nm and the other at 222 nm, an indicative of the helical contents of the protein, were observed in the analysed samples (Fig 4). A decrease in the ellipticity/upward shift in the spectrum at both minima for 3-DG-glycated H1 relative to native H1 was observed. This finding clearly indicates structural alteration or loss of α -helices upon modification by 3-DG [67]. Furthermore, a significant decrease in the T_m of modified histones at 222 nm clearly indicates a decrease in stability/loss of secondary protein structure upon glycation. Some of the interactions that stabilize compact folding conformations are disturbed in modified proteins [67]. This study agrees with previous findings from our laboratory, which demonstrates that glycation reactions and consequent AGE formation has tremendous effect on the functionality and structure of proteins [34].

Native protein structure is maintained by several types of covalent and non-covalent atomic forces. One of the basic biophysical properties of proteins is thermal denaturation vulnerability that governs protein stability and durability, and is altered upon modification [68]. Disturbance in the isoelectric point (pI) of a protein also affects the thermo-stabilizing factors due to change in charges on proteins, leading to reduced protein stability [69]. Lysine and arginine are prime targets of glycation, and are responsible for destabilization of the protein structure. FT-IR identified the structural changes in 3-DG-glycated H1, and is a sensitive technique used to investigate changes in protein structure caused by chemical modification [70]. The shift in band (amide I and amide II) positions as well as augmentation of transmission intensities compared to those of the native conformer clearly demonstrated perturbation of the secondary structure upon modification of H1 by 3-DG.

Taken together, the results of this study confirm that 3-DG is a potential glyating agent that acts through the generation of different intermediates and AGEs that consequently induce structural alteration of H1 protein. Glycation phenomenon occurring in diabetic cases may alter the structure and function of histone proteins, lead to changes in expression of genes, and compromise the function of DNA. These effects may aggravate secondary complications of diabetes. Reactive carbonyl species like glyoxal, MG, and 3-DG present a threat to the cellular system and their biological components like proteins and DNA [71]. Thus, there is a need to quench these reactive carbonyls and glycation using various medicinal plants with anti-oxidant activities [72–76], novel AGE inhibitors [16], and nano-conjugation techniques [61]. Recently, our research group paved the way to study the inhibition of glycation by silver and gold nanoparticles [61, 75]. Apart from gold and silver nanoparticles, a safe and biodegradable gelatin-based drug delivery system can also be used and has produced promising results [76].

Supporting Information

S1 Fig. Procedure of inhibition ELISA for quantification of AGEs formation.
(DOC)

Acknowledgments

The authors thank Yeungnam University (Republic of Korea) as well as the Interdisciplinary Biotechnology Unit of Aligarh Muslim University (India) for providing instruments, facilities, and other items used for this study.

Author Contributions

Conceived and designed the experiments: JMA IC KA RHK SA. Performed the experiments: JMA GR SA. Analyzed the data: JMA SA KA GR. Contributed reagents/materials/analysis tools: JMA SA GR. Wrote the paper: JMA QH IC SA.

References

1. Ahmad S, Dixit K, Shahab U, Alam K, Ali A. Genotoxicity and immunogenicity of DNA-advanced glycation end products formed by methylglyoxal and lysine in presence of Cu^{2+} . *Biochem Biophys Res Commun*. 2011; 407(3): 568–574. doi: [10.1016/j.bbrc.2011.03.064](https://doi.org/10.1016/j.bbrc.2011.03.064) PMID: [21420380](https://pubmed.ncbi.nlm.nih.gov/21420380/)
2. Imteyaz M, Ahmad S, Moinuddin. Preferential recognition of methylglyoxal modified calf thymus DNA by circulating autoantibodies in cancer patients. *Indian J Biochem Biophys*. 2011; 48:290–296.
3. Ashraf JM, Arif B, Dixit K, Moinuddin, Alam K. Physicochemical analysis of structural changes in DNA modified with glucose. *Int J Biol Macro*. 2012; 51(4):604–611.
4. Mustafa I, Ahmad S, Dixit K, Moinuddin, Ahmad J, Ali A. Glycated human DNA is a preferred antigen for anti-DNA antibodies in diabetes mellitus patients. *Diabetes Res Clin Pract*. 2012; 95:98–104. doi: [10.1016/j.diabres.2011.09.018](https://doi.org/10.1016/j.diabres.2011.09.018) PMID: [22001283](https://pubmed.ncbi.nlm.nih.gov/22001283/)
5. Akhter F, Khan MS, Shahab U, Moinuddin, Ahmad S. Bio-physical characterization of ribose induced glycation: A mechanistic study on DNA perturbations. *Int J Biol Macro*. 2013; 58:206–210.
6. Ahmad S, Akhter F, Shahab U, Moinuddin, Khan MS. Studies on Glycation of Human Low Density Lipoprotein: A functional insight into Physico-chemical analysis. *Int J Biol Macro*. 2013; 62:167–71.
7. Akhter F, Khan MS, Ahmad S. Acquired immunogenicity of calf thymus DNA and LDL modified by D-ribose: A comparative study. *Int J Biol Macro*. 2014; 72:1222–1227.
8. Akhter F, Khan MS, Singh S, Ahmad S. An Immunohistochemical analysis to validate the rationale behind the enhanced immunogenicity of D-ribosylated low density lipo-protein. *PLoS ONE*. 2014; 9(11): e113144. doi: [10.1371/journal.pone.0113144](https://doi.org/10.1371/journal.pone.0113144) PMID: [25393017](https://pubmed.ncbi.nlm.nih.gov/25393017/)
9. Thorpe SR, Lyons TJ, Baynes JW. Glycation and glycooxidation in diabetic vascular disease. In: KEANEY JF. *Oxidative Stress and Vascular Disease*. (ed) Norwell, MA, Kluwer Academic Publishers; 2000. pp 259–285.
10. Delpierre G, Rider M, Collard F, Stroobant V, Vanstapel F, Santos H, et al. Identification, cloning, and heterologous expression of a mammalian fructosamine-3-kinase. *Diabetes*. 2000; 49:1627–1634. PMID: [11016445](https://pubmed.ncbi.nlm.nih.gov/11016445/)
11. Zyzak D, Richardson J, Thorpe S, Baynes J. Formation of reactive intermediates from Amadori compounds under physiological conditions. *Arch Biochem Biophys*. 1995; 316:547–554. PMID: [7840665](https://pubmed.ncbi.nlm.nih.gov/7840665/)
12. Beisswenger BG, Delucia EM, Lapoint N, Sanford RJ, Beisswenger PJ. Ketosis leads to increased methylglyoxal production on the Atkins diet. *Ann N Y Acad Sci*. 2005; 1043:201–210. PMID: [16037240](https://pubmed.ncbi.nlm.nih.gov/16037240/)
13. Reichard GA Jr., Skutches CL, Hoeldtke RD, Owen OE. Acetone metabolism in humans during diabetic ketoacidosis. *Diabetes*. 1986; 35: 668–674. PMID: [3086164](https://pubmed.ncbi.nlm.nih.gov/3086164/)
14. Turk Z. Glycotoxines, Carbonyl Stress and Relevance to Diabetes and Its Complications. *Physiol Res*. 2010; 59:147–156. PMID: [19537931](https://pubmed.ncbi.nlm.nih.gov/19537931/)
15. Thornalley PJ. Glutathione-dependent detoxification of alpha-oxoaldehydes by the glyoxalase system: involvement in disease mechanisms and antiproliferative activity of glyoxalase I inhibitors. *Chem Biol Int*. 1998; 24:137–151.
16. Ahmad S, Shahab U, Baig MH, Khan MS, Khan M, Sajid, Saeed M, et al. Inhibitory effect of Metformin and Pyridoxamine in the formation of early, intermediate and advanced glycation end-products. *PLoS ONE*. 2013; 8(9):e72128. doi: [10.1371/journal.pone.0072128](https://doi.org/10.1371/journal.pone.0072128) PMID: [24023728](https://pubmed.ncbi.nlm.nih.gov/24023728/)
17. Shahab U, Tabrez S, Khan MS, Akhter F, Khan MS, Saeed M, et al. Immunogenicity of DNA-advanced glycation end product fashioned through glyoxal and arginine in the presence of Fe^{3+} : its potential role in prompt recognition of diabetes mellitus auto-antibodies. *Chem Biol Interact*. 2014; 219:229–240. doi: [10.1016/j.cbi.2014.06.012](https://doi.org/10.1016/j.cbi.2014.06.012) PMID: [24968179](https://pubmed.ncbi.nlm.nih.gov/24968179/)

18. Lal S, Kappler F, Walker M, Orchard T, Beisswenger P, Szwegold B, et al. Quantitation of 3-deoxyglucosone levels in human plasma. *Arch Biochem Biophys*. 1997; 342:254–260. PMID: [9186486](#)
19. Beisswenger P, Lal S, Howell S. Royal Society of Chemistry Cambridge UK pp: 298–303. 1998.
20. Trivedi I, Rai KM, Singh SK, Kumar V, Singh M, Ranjan A, et al. Analysis of histones and histone variants in plants. *Methods Mol Biol*. 2012; 833:225–236. doi: [10.1007/978-1-61779-477-3_14](#) PMID: [22183597](#)
21. Ahmada K, Henikoff S. The histone variant H3.3 marks active chromatin by replication-independent nucleosome assembly. *Mol Cell*. 2002; 9:1191–1200. PMID: [12086617](#)
22. Redon C, Pilch D, Rogakou E, Sedelnikova O, Newrock K, Bonner W Histone H2A variants H2AX and H2AZ. *Curr Opin Genet Dev*. 2002; 12:162–169. PMID: [11893489](#)
23. Shena X, Gorovsky MA. Linker histone H1 regulates specific gene expression but not global transcription in vivo. *Cell*. 1996; 86:475–483. PMID: [8756729](#)
24. Gugliucci A. Advanced glycation of rat liver histone octamers: An in vitro study. *Biochem Biophys Res Commun*. 1994; 203:588–593. PMID: [8074708](#)
25. Gugliucci A, Bendayan M. Histones from diabetic rats contain increased levels of advanced glycation end products. *Biochem Biophys Res Commun*. 1995; 212:56–62. PMID: [7612018](#)
26. Jobsta K, Lakatos A. The liver cell histones of diabetic patients contain glycation endproducts (AGEs) which may be lipofuscin components. *Clin Chim Acta*. 1996; 256:203–204. PMID: [9027431](#)
27. Cervantes-Laurean D, Jacobson EL, Jacobson MK. Glycation and glycoxidation of histones by ADP-ribose. *J Biol Chem*. 1996; 271:10461–10469. PMID: [8631841](#)
28. Liebich HM, Gesele E, Wirth C, Woll J, Jobst K, Lakatos A. Non-enzymatic glycation of histones. *Biol Mass Spectrom*. 1993; 22:121–123. PMID: [8448220](#)
29. Guedes S, Vitorino R, Domingues MRM, Amado F, Domingues P. Glycation and oxidation of histones H2B and H1: in vitro study and characterization by mass spectrometry. *Anal Bioanal Chem*. 2011; 399:3529–3539. doi: [10.1007/s00216-011-4679-y](#) PMID: [21274518](#)
30. Talasz H, Wasserer S, Puschendorf B. Nonenzymatic glycation of histones in vitro and in vivo. *J Cell Biochem*. 2002; 85:24–34. PMID: [11891847](#)
31. Ansari NA, Dash D. Biochemical Studies on Methylglyoxal-Mediated Glycated Histones: Implications for Presence of Serum Antibodies against the Glycated Histones Patients with Type 1 Diabetes Mellitus. *ISRN Biochemistry*. 2013. Pp-5. Available: <http://dx.doi.org/10.1155/2013/198065>.
32. Mir AR, Moin uddin, Alam K, Ali A. Methylglyoxal mediated conformational changes in histone H2A-generation of carboxyethylated advanced glycation end products. *Int J Biol Macro*. 2014; 69:260–266.
33. Ashraf JM, Ahmad S, Rabbani G, Arif T, Lee EJ, Khan RH, et al. Physicochemical analysis of structural alteration and AGEs generation during glycation of H2A histone by 3-Deoxyglucosone. *IUBMB Life*. 2014; 66(10):686–693. doi: [10.1002/iub.1318](#) PMID: [25380060](#)
34. Ashraf JM, Ahmad S, Rabbani G, Arif T, Lee EJ, Khan RH, et al. 3-Deoxyglucosone: A Potential glycat-ing agent accountable for structural alteration in H3 histone protein through generation of different AGEs. *PLoS ONE*. 2015; 10: e0116804. doi: [10.1371/journal.pone.0116804](#) PMID: [25689368](#)
35. Udenfriend S, Stein S, Bohlen P, Dairman W, Weigle M. Fluorescamine: a reagent for assay of amino acids, peptides, proteins, and primary amines in the picomole range. *Science*. 1972; 78:871–872.
36. Lorenzen A, Kennedy SW. A fluorescence-based protein assay for use with a microplate reader. *Anal Biochem*. 1993; 214:346–348. PMID: [8250247](#)
37. Schmitt A, Schmitt J, Munch G., Gasic-Milencovic J. Characterization of advanced glycation end products for biochemical studies: side chain modifications and fluorescence characteristics. *Anal Biochem*. 2005; 338:201–215. PMID: [15745740](#)
38. Smith RE, MacQuarrie R. A sensitive fluorometric method for the determination of arginine using 9,10-phenanthrenequinone. *Anal Biochem*. 1978; 90:246–255. PMID: [727468](#)
39. Ashraf JM, Arif B, Dixit K, Moinuddin, Alam K. Physicochemical analysis of structural changes in DNA modified with glucose. *Int J Biol Macro*. 2012; 51:604–11.
40. Levine RL, Williams J, Stadtman ER, Shacter E. Carbonyl assays for determination of oxidatively modified proteins. *Methods Enzymol*. 1994; 233:346–357. PMID: [8015469](#)
41. Misselwitz J, Franke S, Kauf E, John U, Stein G. Advanced glycation end products in children with chronic renal failure and type 1 diabetes. *Pediatr Nephrol*. 2002; 5:316–321.
42. Ahmed N, Argirov OK, Minhas HS, Cordeiro CA, Thornalley PJ. Assay of advanced glycation endproducts (AGEs): surveying AGEs by chromatographic assay with derivatization by 6-aminoquinolyl-N-hydroxysuccinimidyl-carbamate and application to Nepsilon-carboxymethyl-lysine- and Nepsilon-(1-carboxyethyl)lysine-modified albumin. *Biochem J*. 2002; 364:1–14. PMID: [11988070](#)

43. Nagai R, Matsumoto K, Ling X, Suzuki H, Araki T, Horiuchi S. Glycolaldehyde, a reactive intermediate for advanced glycation end products, plays an important role in the generation of an active ligand for the macrophage scavenger receptor. *Diabetes*. 2000; 49:1714–1723. PMID: [11016456](#)
44. Arfat MY, Ashraf JM, Arif Z, Moinuddin, Alam K. Fine characterization of glycosylated human IgG by biochemical and biophysical methods. *Int J Biol Macro*. 2014; 69:408–15.
45. Rabbani G, Ahmad E, Zaidi N, Fatima S, Khan RH. pH-Induced molten globule state of *Rhizopus niveus* lipase is more resistant against thermal and chemical denaturation than its native state. *Cell Biochem Biophys*. 2012; 11:9335–9339.
46. Ahmad S, Moinuddin, Shahab U, Khan MS, Habeeb S, Alam K, et al. Glycooxidative damage to human DNA: Neo-antigenic epitopes on DNA molecule could be a possible reason for autoimmune response in type 1 diabetes. *Glycobiology*. 2014; 24:281–291. doi: [10.1093/glycob/cwt109](#) PMID: [24347633](#)
47. Zheng N, Yang T, Liang M, Zhang H, Li L, Sunnassee A, et al. Characterization of protein in old myocardial infarction by FTIR micro-spectroscopy. *J Huazhong Univ Sci Technol*. 2010; 30:546–550.
48. Ahmad S, Khan MS, Khan MS, Akhter F, Khan A, Ashraf JM, et al. Glycooxidation of biological macromolecules: A critical approach to halt the menace of glycation. *Glycobiology*. 2014; 24(11):979–990. doi: [10.1093/glycob/cwu057](#) PMID: [24946787](#)
49. Selvin E, Steffes M, Zhu H, Matsushita K, Wagenknecht L, Pankow J, et al. Glycated hemoglobin, diabetes, and cardiovascular risk in non-diabetic adults. *N Engl J Med*. 2010; 362:800–810. doi: [10.1056/NEJMoa0908359](#) PMID: [20200384](#)
50. Ahmad S, Moinuddin, Habib S, Shahab U, Alam K, Ali A. Autoimmune response to AGE modified human DNA: Implications in type 1 Diabetes mellitus. *J Clin Trans Endo*. 2014; 1(3):66–72.
51. Che W, Asahi M, Takahashi M, Kaneto H, Okado A, Higashiyama S, et al. Selective induction of heparin-binding epidermal growth factor-like growth factor by methylglyoxal and 3-deoxyglucosone in rat aortic smooth muscle cells. The involvement of reactive oxygen species formation and a possible implication for atherogenesis in diabetes. *J Biol Chem*. 1997; 272:18453–18459. PMID: [9218489](#)
52. Hamada Y, Nakamura J, Fujisawa H, Yago H, Nakashima E, Koh N. Effects of glycemic control on plasma 3-deoxyglucosone levels in NIDDM patients. *Diabetes Care*. 1997; 20:1466–1469. PMID: [9283799](#)
53. McGhee JD, Felsenfeld G. Nucleosome structure. *Ann Rev Biochem*. 1989; 49:1115–1156.
54. Sperling R, Wachtel EJ. The histones. *Adv Prot Chem*. 1981; 34:1–60.
55. Von Holt C, Strickland WN, Brandt WF, Strickland MS. More histone structures. *FEBS Lett*. 1979; 100:201–208. PMID: [378692](#)
56. Stefek M, Trnkova Z, Krizanova L. 2,4-dinitrophenylhydrazine carbonyl assay in metal-catalysed protein glycooxidation. *Redox Rep*. 1999; 4:43–48. PMID: [10714275](#)
57. Hodge JR. The Amadori rearrangement. *Adv Carbo Chem*. 1955; 10:169–205.
58. Majd AMA, Goodarzi MT, Hassanzadeh T, et al. In Vitro Study of Glycation of Pyruvate Kinase and Its Effect on Activity and Proteolytic Resistance In Absence And Presence Of Aminoguanidine. *J Basic Appl Sci Res*. 2013; 3:878–884.
59. Degenhardt TP, Thorpe SR, Baynes JW. Chemical modification of proteins by methylglyoxal. *Cell Mol Biol (Noisy-le-Grand)*. 1998; 44:1139–1145.
60. Kessel L, Kalinin S, Nagaraj RH, Larsen M, Johansson LB. Time-resolved and steady-state fluorescence spectroscopic studies of the human lens with comparison to argpyrimidine, pentosidine and 3-OH-kynurenine. *Photochem Photobiol*. 2002; 76:549–554. PMID: [12462652](#)
61. Raheem M, Iram S, Khan MS, Shukla AR, Srivastava AK, Ahmad S. Glycation-assisted synthesized gold nanoparticles inhibit growth of bone cancer cells. *Colloids Surf B Biointerfaces*. 2014; 117:473–479. doi: [10.1016/j.colsurfb.2013.12.008](#) PMID: [24368207](#)
62. Shahab U, Moinuddin, Ahmad S, Dixit K, Abbas Abidi SM, Alam K, et al. Acquired immunogenicity of human DNA damaged by N-hydroxy-N-Acetyl-4-aminobiphenyl. *IUBMB Life*. 2012; 64:340–5. doi: [10.1002/iub.1008](#) PMID: [22378795](#)
63. Moinuddin, Dixit K, Ahmad S, Shahab U, Alam K Ali A. Human DNA damage by the synergistic action of 4-Aminobiphenyl and Nitric Oxide: An Immunochemical Study. *Environ Toxicol*. 2014; 29:568–76.
64. Shahab U, Moinuddin, Ahmad S, Dixit K, Ali A. Genotoxic effect of N-hydroxy-4-acetylaminobiphenyl on human DNA: Implications in bladder cancer. *PLoS ONE*. 2013; 8:e53205. doi: [10.1371/journal.pone.0053205](#) PMID: [23382838](#)
65. Ashraf JM, Arfat MY, Arif Z, Ahmad J, Moinuddin, Alam K. A clinical correlation of anti-DNA-AGE auto-antibodies in type 2 diabetes mellitus with disease duration. *Cell Immunol*. 2015; 293:74–79. doi: [10.1016/j.cellimm.2014.12.007](#) PMID: [25577340](#)

66. Schmitt A, Gasic-Milenkovic J, Schmitt J. Characterization of advanced glycation end products: mass changes in correlation to side chain modifications. *Anal Biochem.* 2005; 346:101–106. PMID: [16168380](#)
67. Rabbani G, Ahmad E, Zaidi N, Khan RH. pH-dependent conformational transitions in conalbumin (ovo-transferrin), a metalloproteinase from hen egg white. *Cell Biochem Biophys.* 2011; 61:551–560. doi: [10.1007/s12013-011-9237-x](#) PMID: [21833676](#)
68. Shahab U, Ahmad S, Moinuddin, Dixit K, Habeeb S, Alam K, et al. Hydroxyl radical modification of collagen type II increases its arthritogenicity and immunogenicity. *PLoS ONE.* 2012; 7:e31199. doi: [10.1371/journal.pone.0031199](#) PMID: [22319617](#)
69. Fojo AT, Whitney PL, Awad WM Jr. Effects of acetylation and guanidination on alkaline conformations of chymotrypsin. *Arch Biochem Biophys.* 1983; 224:636–642. PMID: [6870281](#)
70. Liu Y, Xie MX, Kang J, Zheng D. Studies on the interaction of total saponins of panax notoginseng and human serum albumin by Fourier transform infrared spectroscopy. *Spectrochim Acta A.* 2003; 59:2747–2758.
71. Ahmad S. Immunogenicity of DNA damage by free radicals and carbonyls: A probable bio-marker for the auto-immune diseases. *J Immun Res.* 2014; 1:1–2.
72. Khan MS, Ansari IA, Ahmad S, Akhter F, Hashim A, Srivastava AK. Chemotherapeutic potential of *Boerhaavia diffusa* Linn: A review. *J App Pharm.* 2013;Sc 3:133–139.
73. Arshya H, Khan MS, Khan MS, Beg MH, Ahmad S. Antioxidant and α -amylase inhibitory property of *Phyllanthus virgatus* L.: An In vitro and molecular interaction study. *Bio Med Res Int.* 2013. Available: <http://dx.doi.org/10.1155/2013/729393>.
74. Akhter F, Hashim A, Khan MS, Ahmad S, Iqbal D, Srivastava AK, et al. Antioxidant, α -Amylase Inhibitory and Oxidative DNA Damage Protective Property of *Boerhaavia diffusa* (Linn.) Root South African *J Bot.* 2013; 88:265–272.
75. Ashraf JM, Ansari MA, Choi I, Khan HM, Alzohairy MA. Antiglycating potential of gum arabic capped-silver nanoparticles. *Appl Biochem Biotechnol.* 2014; 174:398–410. doi: [10.1007/s12010-014-1065-1](#) PMID: [25080376](#)
76. Chanchal A, Vohra R, Elesela S, Bhushan L, Kumar S, Kumar S, et al. Gelatin Biopolymer: A Journey from Micro to Nanotechnology. *Journal of Pharm Res.* 2014; 8:1387–1397.